(1)

ANALYSIS OF VOLTAMMETRIC HALF-WAVE POTENTIALS IN LOW IONIC STRENGTH SOLUTIONS
AND
VOLTAMMETRIC MEASUREMENT OF ION IMPURITY CONCENTRATIONS

N00014-84-K-0656

Bradford D. Pendley and Héctor D. Abruña*
Department of Chemistry
Baker Laboratory
Cornell University
Ithaca, NY 14853

ONR

1990

John D. Norton, Wendy E. Benson, and Henry S. White*
Department of Chemical Engineering and Materials Science
University of Minnesota
Minneapolis, MN 55455

ABSTRACT

An analytic equation is presented that allows the prediction of steady-state voltammetric half-wave potentials as a function of electrolyte concentration in low ionic strength solutions for electrodes of arbitrary geometry and size. The equation is tested for the oxidation of ferrocene and reduction of TCNQ in acetonitrile at 2.4 - 22.1 μm platinum microdisk electrodes for electrolyte (tetra-n-butylammonium perchlorate) concentrations between 10^{-1} and 4×10^{-9} M, and in acetonitrile solutions containing no intentionally added electrolyte. An analytical method for measuring ion impurity concentration, based on steady-state microelectrode voltammetry, is proposed and used to measure ionic impurities in acetonitrile. The role of ionic solution impurities on voltammetric measurements in the absence of intentionally added electrolyte is quantified and a criterion for the minimum number of ions required to observe sigmoidally-shaped voltammetric curves at microelectrodes is proposed.

Availability Codes

Dist	Avail and/or Special
A-1	

1

90 12 10 147

INTRODUCTION

There has been considerable recent interest in the use of microelectrodes to study electrochemical reactions in the absence of any deliberately added electrolyte[1-3]. Such endeavors result from a general interest in extending the scope of electrochemical measurements to solvents in which electrolytes are insoluble or to systems in which electrolyte ions interfere with quantitative voltammetric analyses. Performing electrochemistry in the absence of an electrolyte also raises fundamental questions regarding the assumed role of the supporting electrolyte in charge-transport mechanisms, and in establishing electric fields at the electrode/electrolyte interface.

The oxidation of ferrocene (Fc) in acetonitrile (CH_3CN), eq. (1), under steady-state conditions at microdisk

$$Fc \rightleftharpoons Fc^+ + e^- \qquad (1)$$

electrodes has been frequently used to demonstrate the feasibility of performing electrochemistry without an added electrolyte[4-8]. A sigmoidally-shaped voltammogram is observed in the absence of electrolyte, with shape and magnitude that are similar to those obtained in the presence of high concentrations of electrolyte. As noted by Oldham[9], the ability to observe a sigmoidal voltammetric response at a microelectrode in solutions of low ionic strength is a result of the convergent fluxes of the redox species and supporting electrolyte ions to the electrode. These convergent fluxes create higher, albeit non-uniform, concentrations of ionic species within the depletion layer surrounding the microelectrode when compared to those present in the bulk of the solution. A consequence of these increases in ionic concentrations is that the resistivity of the solution adjacent to the electrode is significantly lowered relative to the bulk solution value, allowing voltammetric measurements to be made under conditions that are normally considered to be prohibitively resistive. It is implicitly assumed in Oldham's analysis that a source of counterions is

2

present in the electrochemical cell in order to maintain electroneutrality throughout the solution (neglecting charge separation within the double layer). In the absence of an electrolyte, the requisite counterions necessary to balance the charge generated at the microelectrode may, in principle, be simultaneously produced at the counterelectrode by faradaic reactions or it may be assumed, for the sake of mathematical analyses, that there is an infinite volume of solution which contains some small but non-zero concentration of bulk electrolyte. In practice, the former means of charge balance (counterelectrode generation) would require transport of counterions from the counterelectrode to the working microelectrode on time scales comparable to the voltammetric experiment. In most instances, such a means of charge balance would require migration/diffusion of ions over distances ranging from several millimeters to centimeters in tens of seconds or less, an unrealistically large rate. The second method of maintaining charge balance, based on the assumption of an infinitely large volume of solution containing a finite concentration of ions, is, of course, a mathematical convenience, but leads to difficulties in defining a working value of the minimum ion concentration necessary to observe a voltammetric response. As will be developed in this paper, the ability to observe sigmoidally shaped voltammograms requires a minimum *number* of solution ions, determined by both the electrolyte concentration (including impurity ions) and volume of the electrochemical cell.

Bond, Peña, Amatore, and coworkers[4-7] have observed that the voltammetric half-wave potential, $E_{1/2}$, for ferrocene oxidation shifts towards positive potentials with decreasing electrolyte concentration, while Kamau and Rusling[10] observed negative shifts in $E_{1/2}$ for the reduction of TCNQ with decreasing electrolyte concentration. They ascribe these dependencies, in part, to ohmic drop and variations in the liquid junction potential at the reference electrode/electrolyte interface, although no data were presented to directly support these claims. Oldham's[9] theoretical analysis of voltammetry at *microhemispherical* electrodes in solutions of low ionic strength, provides an analytic expression relating $E_{1/2}$ for ferrocene oxidation to the supporting electrolyte concentration. To our knowledge, this

relationship has not been rigorously tested, although it appears to be in good qualitative agreement with the earlier experimental results of Bond et al.[4,5], Peña et al.[6] and Amatore et al.[7] Oldham's analysis also does not explicitly include the role of ionic impurities, which would be expected to play a predominant role in determining $E_{1/2}$ in solutions containing a very small quantity of an added supporting electrolyte.

In this report, an analytic expression for voltammetric $E_{1/2}$ values in low ionic strength solutions is derived for electrodes of arbitrary geometry at which a true steady-state voltammetric response is obtained (e.g., microdisk electrode, rotating disk electrode, etc.). As shown in the Results and Discussion section, this expression is a generalization of the equation derived by Oldham assuming a hemispherical geometry. The validity of the equation is experimentally tested by measurements of $E_{1/2}$ as a function of supporting electrolyte concentration for ferrocene oxidation and TCNQ reduction in CH_3CN. We show that at very low levels of supporting electrolyte, $E_{1/2}$ becomes independent of the supporting electrolyte concentration and is controlled by the background impurity ion concentration. Finally, we propose that a minimum *absolute number* of ions, resulting from either the deliberate addition of supporting electrolyte or from impurities, is necessary to observe a conventional voltammetric response at a microdisk electrode. This value is compared to examples in the literature in which "electrochemistry without electrolyte" is described. A general conclusion of this work is that the solutions employed in this study, and most likely those used in other experiments reported in the literature, contain sufficient ionic impurities to easily satisfy physical conditions necessary to observe a sigmoidal voltammetric response in the absence of a deliberately added supporting electrolyte.

EXPERIMENTAL

Acetonitrile (Burdick and Jackson Distilled in Glass) was dried over 4 Å molecular sieves. Ferrocene (Fc, Aldrich 98%) and tetracyanoquinodimethane (TCNQ, Aldrich 98%) were used as received. Tetra-n-butylammonium perchlorate (TBAP, GF Smith) was

4

recrystallized three times from ethyl acetate and dried under vacuum. Water was purified with a Millipore Milli-Q system. All other reagents were of at least reagent grade quality and were used without further purification.

Platinum microdisk electrodes were prepared by two methods. In the first, a 2 cm length of nominally 2.5 μm radius Pt wire (Goodfellow, 99.9%, purchased as Wollaston wire) or 12.5 μm radius Pt wire (AESAR, 99.95%) was attached to the end of a copper wire with silver paint. The silver coating on the Wollaston wire was removed by dipping the wire in concentrated nitric acid followed by rinsing the wire with water. The Pt wire was sealed inside a 3mm o.d. glass tube with an oxygen-gas flame. Electrical contact to an external wire was made using a drop of mercury. The tip of the electrode was successively polished with 400 and 600 grit sandpaper to expose the platinum wire. Optical microscopy was used to identify electrodes with imperfect seals at the Pt/glass interface. The second construction method consisted of sealing a previously constructed microelectrode[11] in a 3mm o.d. glass tube and polishing with 400 and 600 grit sandpaper. Prior to each experiment, the electrode was polished with 1 μm diamond paste (Buehler). Similar results were obtained using both methods of electrode construction. Precise values of the electrode radii were calculated from values of the steady-state voltammetric limiting currents for the oxidation of 1mM ferrocene in acetonitrile containing 0.1M TBAP and using the reported value for the diffusivity of ferrocene in acetonitrile (2.4×10^{-5} cm^2/s)[12].

Electrochemical measurements were made using a conventional three-compartment cell (4 cm^3 volume). All potentials were measured versus a sodium-saturated calomel electrode (SSCE). Cyclic voltammetric experiments were performed with an IBM EC/225 voltammetric analyzer and were recorded on a Soltec VP-6423S X-Y recorder. Voltammetric measurements were conducted with the electrochemical cell inside a Faraday cage and were performed at $22 \pm 0.2°$ C.

RESULTS AND DISCUSSION.

Derivation of the Dependence of $E_{1/2}$ on Electrolyte Concentration.

Oldham has previously derived an expression for the dependence of voltammetric $E_{1/2}$ values on electrolyte concentration for the special case of a hemispherical electrode. The following analysis, which leads to an identical expression in the limit of very low electrolyte concentrations, requires no assumptions regarding electrode geometry or size. The result allows the extension of $E_{1/2}$ analyses to microdisk electrodes which are significantly simpler to construct than hemispherical electrodes.

The one-electron reduction of a neutral redox species, A,

$$A + e^- \rightleftharpoons A^- \tag{2}$$

in a solution containing A and a 1:1 electrolyte, X^+Y^-, at their respective bulk concentrations C_A^*, $C_{X^+}^*$, and $C_{Y^-}^*$ will be considered. The product, A^-, is initially absent from solution, so its bulk concentration, $C_{A^-}^*$, is zero. A large, non-polarizable electrode serves as both a reference and counterelectrode and is positioned at a large distance from the working electrode.

Reaction (2) is assumed to be electrochemically reversible. The potential of the working electrode, E, measured relative to the reference electrode, is thus given by

$$E = E^{o'} + \frac{RT}{F} \ln\left(\frac{C_A^s}{C_{A^-}^s}\right) + (\phi^s - \phi^*) + \Delta\phi_{ref} \tag{3}$$

where $E^{o'}$ is the formal potential of reaction (2), C_A^s and $C_{A^-}^s$ are the surface concentrations of A and A^-, respectively, $\Delta\phi_{ref}$ is the potential drop across the reference electrode/electrolyte interface, ϕ^s is the potential in solution directly adjacent to the working

6

electrode surface, ϕ^* is the potential in the bulk solution far away from the working electrode, and all other symbols have their usual meaning. We assume that $\Delta\phi_{ref}$ is a constant, independent of electrolyte concentration. Although strictly not true, this assumption, which appears to be a source of confusion in previous analyses of voltammetric measurements in low ionic strength solutions, will be demonstrated to be valid for the experiments presented below. The quantity $(\phi^s - \phi^*)$ in eq. (3) represents the ohmic potential drop in solution resulting from the passage of a finite current.

The current, I, corresponding to the reduction of A is given by

$$I = m_A nF\mathcal{A}(C_A^* - C_A^S)$$ (4)

or by

$$I = m_{A^-} nF\mathcal{A}\, C_{A^-}^S$$ (5)

where m_A and m_{A^-} denote the mass-transfer coefficients of A and A$^-$, respectively, and $\mathcal{A}$ is the area of the working electrode. The values of m_A and m_{A^-} depend on electrode geometry and size, as well as the chemical composition (e.g., ion concentration) and physical properties (e.g., viscosity) of the solution. The mass-transfer limiting current plateau, I_{lim}, occurs at potentials where $C_A^S \rightarrow 0$.

$$I_{lim} = m_A nF\mathcal{A}C_A^*$$ (6)

In the absence of convection, the steady-state fluxes of the four species in solution are given by the Nernst-Planck equation:

$$J_A(r) = -D_A\nabla C_A(r)$$ (7)

7

$$J_{A^-}(\mathbf{r}) = -D_{A^-}\nabla C_{A^-}(\mathbf{r}) + \frac{F}{RT}D_{A^-}C_{A^-}(\mathbf{r})\nabla\phi(\mathbf{r}) \tag{8}$$

$$J_{X^+}(\mathbf{r}) = -D_{X^+}\nabla C_{X^+}(\mathbf{r}) - \frac{F}{RT}D_{X^+}C_{X^+}(\mathbf{r})\nabla\phi(\mathbf{r}) \tag{9}$$

$$J_{Y^-}(\mathbf{r}) = -D_{Y^-}\nabla C_{Y^-}(\mathbf{r}) + \frac{F}{RT}D_{Y^-}C_{Y^-}(\mathbf{r})\nabla\phi(\mathbf{r}) \tag{10}$$

where $-\nabla\phi(\mathbf{r})$ is the electric field at a position $\mathbf{r}$.

At steady-state, the fluxes of the electrolyte ions are zero, i.e., $J_{X^+}(\mathbf{r}) = J_{Y^-}(\mathbf{r}) = 0$. Substitution of this condition into eq. (9) yields

$$\nabla\phi(\mathbf{r}) = -\frac{RT}{F}\frac{\nabla C_{X^+}(\mathbf{r})}{C_{X^+}(\mathbf{r})} \tag{11}$$

which can be integrated between the limits

$$\phi(\mathbf{r}) = \phi^s \text{ and } C_{X^+}(\mathbf{r}) = C_{X^+}^s \text{ at } \mathbf{r} = \mathbf{r}^s \tag{12}$$

$$\phi(\mathbf{r}) = \phi^* \text{ and } C_{X^+}(\mathbf{r}) = C_{X^+}^* \text{ at } \mathbf{r} \to \infty \tag{13}$$

to yield

$$\phi^s - \phi^* = \frac{RT}{F}\ln\left(\frac{C_{X^+}^*}{C_{X^+}^s}\right) \tag{14}$$

where $\mathbf{r}^s$ is the position vector in the solution directly adjacent to the electrode surface. Substitution of eqs. (4) - (6) and (14) into eq. (3) gives

$$E = E^{o'} + \frac{RT}{F}\ln\left(\frac{m_{A^-}}{m_A}\frac{I_{lim} - I}{I}\right) + \frac{RT}{F}\ln\left(\frac{C_{X^+}^*}{C_{X^+}^s}\right) + \Delta\phi_{ref} \tag{15}$$

8

It is important to note at this point that no constraints have been placed on the electrode geometry nor the values of the mass-transfer coefficients.

In the presence of excess electrolyte (relative to the total concentration of redox active species) the ohmic potential drop in the depletion layer is vanishingly small, i.e., $(\phi^s - \phi^*) \to 0$ and $C_{X^+}^s \approx C_{X^+}^*$ when $C_{X^+}^*/C_A^* \gg 1$. In this limit, eq. (15) becomes

$$E = E_{1/2}(\text{excess electrolyte}) + \frac{RT}{F}\ln\left(\frac{I_{lim} - I}{I}\right) + \Delta\phi_{ref} \qquad (16)$$

where

$$E_{1/2}(\text{excess electrolyte}) = E^{o'} + \frac{RT}{F}\ln\left(\frac{m_A'-}{m_A'}\right) \qquad (17)$$

The halfwave potential, $E_{1/2}$, is defined as the potential at which the current, I, is equal to one-half of the mass-transfer limited current, I_{lim}, (i.e., $I = 1/2\ I_{lim}$). The primes used in the notation of the mass-transfer coefficients indicate that these values are obtained in the presence of excess supporting electrolyte.

When the concentration of supporting electrolyte is comparable to or smaller than that of the redox species, the term $\frac{RT}{F}\ln(C_{X^+}^*/C_{X^+}^s)$ will have a finite value. Eq. (15) then becomes

$$E = E_{1/2} + \frac{RT}{F}\ln\left(\frac{I_{lim} - I}{I}\right) + \Delta\phi_{ref} \qquad (18)$$

where $E_{1/2}$ is defined as

$$E_{1/2} = E^{o'} + \frac{RT}{F}\ln\left(\frac{m_A''- \ C_{X^+}^*}{m_A''\ C_{X^+}^s}\right) \qquad (19)$$

9

and where the double primes on the mass-transfer coefficients indicate values obtained in the absence of excess supporting electrolyte.

The shift in $E_{1/2}$ when $C_A^* \geq C_{X^+}^*$, relative to the value in the presence of excess supporting electrolyte, is obtained by subtracting eq. (19) from eq.(17).

$$E_{1/2}(\text{excess electrolyte}) - E_{1/2} = \frac{RT}{F} \ln \left(\frac{m_A^{'} \cdot m_A^{''} \, C_{X^+}^{s}}{m_A^{'} \, m_{A^-}^{''} \, C_{X^+}^{*}} \right) \qquad (20)$$

In order to compare eq. (20) to experimental results, the relationship between the mass-transfer coefficients $m_A^{'}$, $m_A^{''}$, $m_{A^-}^{'}$, and $m_{A^-}^{''}$ as well as the surface concentration of X^+ must be specified.

In solutions containing excess supporting electrolyte, the electric field term, $-\nabla\phi(\mathbf{r})$, in eqs. (7) - (10) is negligibly small, allowing eq. (8) to be simplified to

$$\mathbf{J}_{A^-}(\mathbf{r}) = -D_{A^-} \cdot \nabla C_{A^-}(\mathbf{r}) \qquad (21)$$

A mass balance at steady-state requires $\mathbf{J}_{A^-}(\mathbf{r}) = -\mathbf{J}_A(\mathbf{r})$. Combining this latter condition with eqs. (7) and (21) yields

$$\nabla C_A(\mathbf{r}) = -\frac{D_{A^-}}{D_A} \nabla C_{A^-}(\mathbf{r}) \qquad (22)$$

which, when integrated between the electrode surface ($\mathbf{r} = \mathbf{r}^s$) and the bulk solution ($\mathbf{r} \rightarrow \infty$) gives

$$C_A^* - C_A^s = \frac{D_{A^-}}{D_A} C_{A^-}^s \qquad (23)$$

Combining eq.(23) with eqs. (4) and (5) yields

$$\frac{D_{A^-}}{D_A} \simeq \frac{m'_{A^-}}{m'_A} \tag{24}$$

where the primed notation is again used to indicate mass-transfer coefficients evaluated when excess supporting electrolyte is present in the solution.

In solutions in which little electrolyte is present, the migrational fluxes in eqs. (7) - (10) cannot be neglected. At the electrode surface, electroneutrality is maintained by the migration of X^+ inward from the bulk. Expulsion of Y^- also occurs, so that its concentration is negligibly small near the electrode surface. Thus, for $C_{X^+}^*/C_A^* \ll 1$

$$C_{X^+} \simeq C_{A^-} \tag{25}$$

$$\nabla C_{X^+}(\mathbf{r}) \simeq \nabla C_{A^-}(\mathbf{r}) \tag{26}$$

Eqs. (25) and (26) are justified when the current, I, represents some significant fraction of I_{lim}. At very small currents (at the foot of the voltammetric wave) the contribution of Y^- to the overall charge balance must be considered.

Combining eqs. (8), (9), (25) and (26) and noting again that $J_{X^+}(\mathbf{r}) = 0$ at steady-state, yields

$$J_{A^-}(\mathbf{r}) = -(2D_{A^-})\nabla C_{A^-}(\mathbf{r}) \tag{27}$$

Again using the mass balance $J_A(\mathbf{r}) = -J_{A^-}(\mathbf{r})$, eqs. (27) and (7) may be combined and integrated between the surface and the bulk solution to yield

$$C_A^* - C_A^s = \frac{2D_{A^-}}{D_A} C_{A^-}^s \tag{28}$$

Substitution of equation (28) into eqs. (4) and (5) yields

11

$$\frac{m_A^{''}}{m_A^{''}} = \frac{2D_{A^-}}{D_A} \qquad (29)$$

Combining eqs. (24) and (29) yields

$$\frac{m_A^{'} \cdot m_A^{''}}{m_A^{'} \, m_{A^-}^{''}} = \frac{1}{2} \qquad (30)$$

The surface concentration of electrolyte cation, $C_{X^+}^s$, to be used in eq. (20) can be found by combining eqs. (25) and (28) and noting that at $E_{1/2}$, $C_A^s = \frac{1}{2} C_A^*$, to give

$$C_{X^+}^s = \frac{C_A^*}{4} \frac{D_A}{D_{A^-}} \qquad (31)$$

Substitution of the expression for $C_{X^+}^s$ at $E_{1/2}$ (eq. (31)) and the mass-transfer coefficients (eq. (30)) into eq. (20) gives

$$E_{1/2}(\text{excess electrolyte}) - E_{1/2} = \frac{RT}{F} \ln\left(\frac{1}{8} \frac{C_A^*}{C_{X^+}^*} \frac{D_A}{D_{A^-}} \right) \qquad (32)$$

A similar analysis yields

$$E_{1/2}(\text{excess electrolyte}) - E_{1/2} = -\frac{RT}{F} \ln\left(\frac{1}{8} \frac{C_A^*}{C_{Y^-}^*} \frac{D_A}{D_{A^+}} \right) \qquad (33)$$

for the one-electron oxidation of A ($A \rightleftarrows A^+ + e^-$).

Eqs. (32) and (33) indicate that steady-state sigmoidal voltammograms for the one-electron reduction and oxidation of a neutral species will shift towards negative and positive potentials, respectively, at a rate of 58 mV (at 22°C) per decade change in supporting electrolyte concentration, in solutions in which the concentration of A remains constant.

The useful working range of eqs. (32) and (33) is bound by both experimental and theoretical considerations, discussed briefly in the following paragraphs.

(i) *Minimum Electrolyte Concentration.* At very low concentrations of added supporting electrolyte, C_{Y-}^* and C_{X+}^* are determined by the sum of the concentration of added supporting electrolyte, C_{elec}, and the concentration of impurities in the bulk of the solution that can serve as an electrolyte, C_{imp}^*. We will assume for simplicity that all ionic impurities are 1:1 electrolytes. Thus, for the one-electron reduction of a neutral species at low concentrations of supporting electrolyte, eq.(32) becomes

$$E_{1/2} \text{ (excess electrolyte)} - E_{1/2} = \frac{RT}{F} \ln\left(\frac{C_A^* D_A}{8(C_{elec}^* + C_{imp}^*)D_{A-}}\right) \qquad (34)$$

and for a one-electron oxidation, eq. (33) becomes

$$E_{1/2} \text{ (excess electrolyte)} - E_{1/2} = -\frac{RT}{F} \ln\left(\frac{C_A^* D_A}{8(C_{elec}^* + C_{imp}^*)D_{A+}}\right) \qquad (35)$$

Eqs. (34) and (35) suggest that voltammetric $E_{1/2}$ values should be independent of electrolyte concentration, C_{elec}^*, in solutions in which the electrolyte concentration is lower than the ion impurity concentration, (i.e. when $C_{imp}^* \gg C_{elec}^*$). We show below that this result can be used to estimate the concentration of impurity ions.

(ii) *Maximum Electrolyte Concentration.* In deriving eq. (32), we assumed that electroneutrality was maintained within the depletion layer by the product anion (A⁻) and the electrolyte cation (X⁺) (see eq. (25) and the preceding discussion). We state, without proof, that the surface concentrations of A⁻ and X⁺ at a hemispherical electrode are equal within 1% when $C_A^* > 36\ C_{elec}$, a result obtained from algebraic manipulation of eqs. (19),

13

(26), and (27) in Oldham[9]. These latter equations give explicit expressions for the concentrations profiles of redox species and electrolyte ions surrounding a hemispherical electrode in the limit of low electrolyte concentration. Slightly different relative concentrations of A and electrolyte are expected to satisfy this criterion for different electrode geometries, including the microdisk electrode employed in the present work. A precise value of the maximum electrolyte concentration allowable in the analysis of voltammetric $E_{1/2}$ values using microdisk electrodes, however, is not crucial in tne analysis of the experimental results and has not been pursued.

For completeness, it is worth comparing the above results for an arbitrary electrode geometry with that derived by Oldham assuming a hemispherical electrode[9]. For the one-electron oxidation of a neutral species, Oldham gives (using our notation):

$$E^o - E_{1/2} = -\frac{RT}{F} \ln \left(\frac{D_A}{D_{A^+}} \left[1 + \frac{D_A C_A^*}{8 D_{A^+} C_{Y^-}^*} \right] \right) \qquad (36)$$

which, after substitution of $E_{1/2}$ (excess electrolyte) $= E^o + \frac{RT}{F} \ln \frac{D_A}{D_{A^+}}$, is identical to eq. (33) in the limit of $C_A^* \gg C_{Y^-}^*$. Eq. (36) is more general than eq. (33) in that it is also applicable to solutions in which the supporting electrolyte is present at excess concentrations. The fact that eqs. (33) and (36) coincide at low electrolyte concentrations, however, does not verify the applicability of eq. (36) for microdisk electrodes at high electrolyte concentrations.

Voltammetric Oxidation of Ferrocene in Low Ionic Strength Solutions.

Voltammograms were obtained for the oxidation of 1mM ferrocene in CH_3CN containing TBAP at concentrations ranging from 0.1 M to 4 nM. Representative voltammograms are shown in Figure 1. Voltammograms were obtained using Pt microdisk electrodes of 2.4, 12.4, 21.3 and 22.1µm radii at a scan rate of 20mV/s. In agreement with previous studies, we find that sigmoidally-shaped voltammograms can be obtained

14

for ferrocene oxidation in CH_3CN solutions containing very little supporting electrolyte and in solutions containing no deliberately added electrolyte.

Experimental values of $E_{1/2}$ are shown in Fig. 2 for the oxidation of ~1 mM Fc. The results are plotted as $(E_{1/2}(xs.\ elec.) - E_{1/2})$ vs $\ln(C_{redox}/8C_{elec})$, where $E_{1/2}(xs.\ elec.)$ is arbitrarily defined as the value of $E_{1/2}$ in CH_3CN containing 0.1 M TBAP. The latter value is equal to 0.40_8 V vs. SSCE. The plot shows three distinct regions. (i) In solutions containing excess supporting electrolyte, $C_{Fc}/C_{TBAP} << 1$, $E_{1/2}$ is essentially independent of TBAP concentration. (ii) For values of C_{Fc}/C_{TBAP} between 10 and 1000, a linear dependence of $(E_{1/2}(xs.\ elec.) - E_{1/2})$ on $\ln(C_{Fc}/8C_{TBAP})$ is observed with a slope of -24.7 mV. (iii) For C_{Fc}/C_{TBAP} values greater than 5000, $(E_{1/2}(xs.\ elec.) - E_{1/2})$ is again independent of C_{Fc}/C_{TBAP} and is equal to -208 ± 38 m . This last value is within experimental error of $(E_{1/2}(xs.\ elec.) - E_{1/2})$ for ferrocene oxidation measured in the absence of any added supporting electrolyte, -209 ± 27 mV.

The experimental data in Fig. 2 for ferrocene oxidation are in quantitative agreement with expectations based on eq. (35) which predicts a slope of -25.3mV for a plot of $(E_{1/2}(xs.\ elec.) - E_{1/2})$ versus $\ln(C_{Fc}/8C_{TBAP})$ between the limits $C_{Fc}/C_{TBAP} > 1$ and $C_{imp}/C_{TBAP} < 1$. In solutions in which the ionic impurity concentration exceeds that of TBAP, eq. (35) reduces to

$$E_{1/2}\ (\text{excess electrolyte}) - E_{1/2} = -\frac{RT}{F}\ln\left(\frac{C_A{}^*D_A}{8C_{imp}{}^*D_{A^+}}\right) \qquad (37)$$

From the measured values of $E_{1/2}$ in the absence of supporting electrolyte we calculate, using equation (37), that the ion impurity concentration in our cell is between 40 and 170 nM (assuming equal diffusivities for ferrocene and ferricenium) or between 80 and 340nM (assuming that the diffusivity of ferrocene is twice the value for ferricenium). While we were unable to measure a diffusion coefficient for ferricenium in acetonitrile due to its rapid

15

decomposition, we note that Ruff et al.[13] measured the diffusion coefficient for ferrocene and ferricenium in methanol, ethanol, and 1-propanol and obtained relative diffusivities for ferrocene to ferricenium of 1.62, 2.23, and 4.57, respectively. Using an impurity concentration of 40nM and assuming equal diffusivities for ferrocene and ferricenium, we have fit the voltammetric data to eq. (35), which is shown as the dashed line in Fig. 2. Using an impurity concentration of 80nM and assuming that the diffusion coefficient for ferrocene is twice that of ferricenium, we have fit the voltammetric data to eq. (35), which is shown as the solid line in Fig. 2. Good agreement between theory and experiment is obtained for $C_{Fc}/C_{TBAP} \geq 25$ and assuming different diffusivities for ferrocene and ferricenium. We believe this assumption is reasonable based on the work of Ruff et al.[13]. Notice that there is no predicted dependence of $E_{1/2}$ on electrode radius (eq. (35)), and none was observed for electrodes with radii between 2.4 and 22.1 μm.

A similar set of measurements of voltammetric $E_{1/2}$ values were performed for the reduction of TCNQ to demonstrate that the experimental slope is not a result of a variation in the liquid junction potential at the reference electrode/electrolyte interface. TCNQ undergoes a one-electron reduction to the corresponding radical anion (TCNQ + $e^- \rightleftharpoons$ TCNQ$^-$) and thus, the appropriate equation for the analysis of voltammetric $E_{1/2}$ values is eq. (34) which predicts that a plot of $(E_{1/2}(xs.\ elec.) - E_{1/2})$ vs. $\ln(C_{TCNQ}/8C_{TBAP})$ should have a *positive* slope of 25.3 mV. Voltammograms for the reduction of TCNQ at a 21.3μm Pt microdisk electrode were obtained in CH$_3$CN containing different concentrations of TBAP and analyzed by a similar procedure as described for the ferrocene data (assuming equal diffusivities). Values of $E_{1/2}$(excess electrolyte) = + 0.220 V vs SSCE and $C_{imp}^* = 260$ nM were obtained from voltammetry in CH$_3$CN solutions containing 0.1 M TBAP and no added electrolyte, respectively. Using these data, good agreement between the predicted and experimental shifts in $E_{1/2}$ values are observed (dashed line, Fig. 2). For values of $C_{TCNQ}/C_{TBAP} \geq 1700$, $(E_{1/2}(xs.\ elec.) - E_{1/2})$ is independent of C_{TCNQ}/C_{TBAP} and is equal to 122 $\pm$ 31 mV. This value is within the

16

experimental error for $(E_{1/2}(\text{xs. elec.}) - E_{1/2})$ for TCNQ reduction in the absence of any added supporting electrolyte, 136 ± 27 mV. It is highly unlikely that **both positive** and **negative** slopes of the correct predicted magnitude could be obtained for TCNQ reduction and ferrocene oxidation as a result of changes in the liquid junction potential. We conclude that variations in the liquid junction potential are small relative to variation in $E_{1/2}$ due to ohmic polarization.

The sources of impurities that can act as electrolyte are not known with certainty, however, the two obvious sources of impurities are the solvent and the redox species. We note that the measured impurity level in solution for one lot of TCNQ was 6μM while for another it was only 260nM using the same solvent, and that these levels differ from the ferrocene impurity concentration, implying that, in this instance, the redox species provided the major source of impurity.

A Criterion for Observing Sigmoidally-Shaped Voltammetric Waves

As previously shown by Morris[14] et al., the minimum theoretical quantity of supporting electrolyte anion, $N(\delta)$ (mole), required to balance the faradaic charge within the depletion layer resulting from oxidation of a neutral species can be estimated by integrating the steady-state concentration profiles of the product ion , (e.g., Fc$^+$) in eq. (1). At potentials corresponding to the migration-diffusion limited current plateau at a hemispherical electrode, this integration is readily performed to yield

$$N(\delta) = \frac{1}{2}\pi C^* r_o{}^3 (\delta^2 - 1) \qquad (38)$$

where r_o is the radius of the microdisk, C^* is the concentration of the redox species generating the Faradaic current, and δ is the thickness of the depletion layer normalized to the electrode radius, r_o. Because of the divergent fluxes of product ions away from a hemispherical electrode, the depletion layer thickness is relatively small, on the order of

$10r_o$. Thus, using $\delta = 10$, eq. (38) provides an estimate of the amount of product ion within the depletion layer at steady-state. $N(\delta)$ also corresponds to the sum of the number of moles of electrolyte anions that must migrate inwards towards the electrode plus the number of electrolyte cations that are expelled to maintain charge balance within the depletion layer. In solutions in which the electrolyte is present at significantly lower concentration than the neutral redox species, charge balance is maintained almost entirely by the inward migration of the electrolyte anion since the total quantity of electrolyte cation within the depletion layer is negligible relative to the quantity of product cations produced at the limiting current plateau.

If the quantity of electrolyte anions in the solution is less than $N(\delta)$, it will be theoretically impossible to maintain electroneutrality within the depletion layer. Thus, a sigmoidally shaped voltammetric wave, which is the result of the potential dependent fluxes of both neutral reactant, cation product, and electrolyte ions (assuming electroneutrality), will not be obtained. We thus propose that $N(\delta)$ may be used to estimate the minimum quantity of electrolyte necessary to establish a voltammetric limiting current and that the criterion for observing a conventional voltammetric response is

$$N_{elec} \gg N(\delta) \tag{39}$$

where N_{elec} is the total number of moles of electrolyte within the cell.

In the experiments described above, approximately 2×10^{-15} mole of supporting electrolyte anion (ClO_4^-) must migrate from the bulk solution to balance the steady-state charge resulting from the oxidation of 1mM ferrocene at a 2.4 μm electrode. The corresponding number for voltammetry at a 22.1 μm radius electrode is 2×10^{-12} moles. With a cell volume of 4 cm^3, this suggests that the electrolyte concentration necessary to balance the steady-state charge is between $\sim 0.5\text{-}400 \times 10^{-12}$ M. Since the ion impurity concentration estimated from voltammetric $E_{1/2}$ values in the absence of electrolyte is over

two orders of magnitude greater than these values, the impurity ions can be considered to be in excess of the minimum required value.

We note that the shifts in $E_{1/2}$ for ferrocene oxidation in CH_3CN in the absence of electrolyte, relative to $E_{1/2}$ (excess electrolyte), reported by other researchers range from ~ 60-120 mV, significantly less that the shift in $E_{1/2}$ observed in the present studies. This suggests, based on our analyses of $E_{1/2}$ values, that the impurity concentration in those studies is larger than the level determined for our CH_3CN solutions. Thus, assuming that excessively small electrochemical cells were not employed, the quantity of ionic impurities present in these studies also exceed the minimum value (eq. (38)) required to observe a sigmoidally-shaped voltammetric curve.

CONCLUSIONS

The present work extends and verifies the theoretical predictions of Oldham for the variation in $E_{1/2}$ values of steady-state voltammograms as a function of supporting electrolyte concentration to include microelectrodes of arbitrary size and geometry. The experimental results for the oxidation of ferrocene and reduction of TCNQ in CH_3CN are in good agreement with the theoretical predictions presented here, which includes the role of ionic impurities. A voltammetric method has been developed and employed for measuring the background level of impurities that can act as *excess* supporting electrolyte in steady-state voltammetry. The measurements show that the impurity level in these solutions exceeds the minimum quantity necessary for charge compensation in voltammetric measurements of ferrocene oxidation.
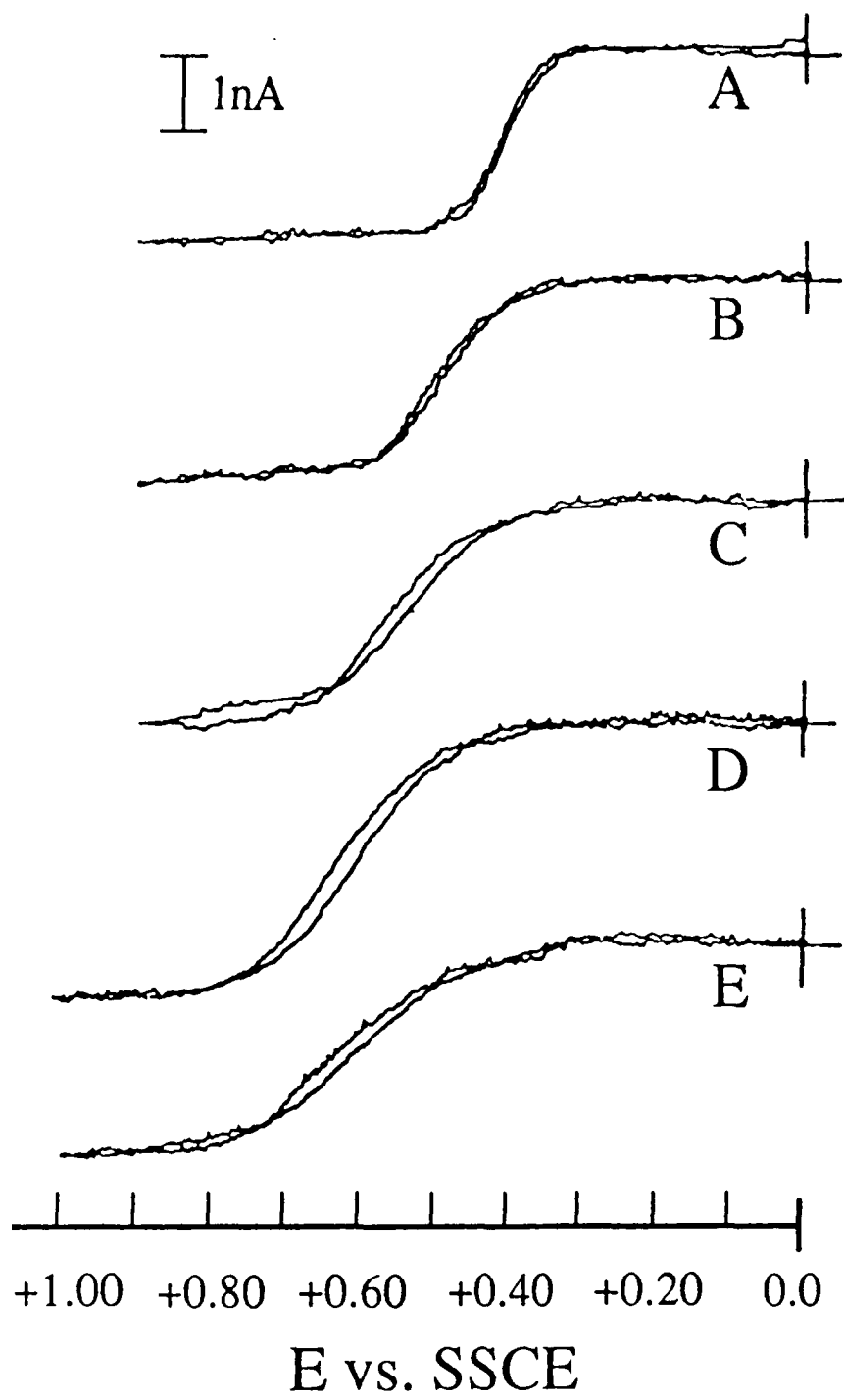
CREDITS

REFERENCES

1. Cassidy, J.; Khoo, S.B.; Pons, S.; Fleischmann, M. *J. Phys. Chem.* **1985**, *89*, 3933-3935.

2. Dibble, T.; Bandyopadhyay, S.; Ghoroghchian, J.; Smith, J.J.; Sarfarazi, F.; Fleischmann, M.; Pons, S. *J. Phys. Chem.* **1986**, *90*, 5275-5277.

3. Ciszkowska, M.; Stojek, Z.; Osteryoung, J. *Anal. Chem.* **1990**, *62*, 349-353.

4. Bond, A.M.; Fleischmann, M.; Robinson, J. *J. Electroanal. Chem.* **1984**, *168*, 299-312.

5. Bond, A.M.; Lay, P.A. *J. Electroanal. Chem.* **1986**, *199*, 285-295.

6. Peña, M.J.; Fleischmann, M.; Garrard, N. *J. Electroanal. Chem.* **1987**, *220*, 31-40.

7. Amatore, C.; Deakin, M.R.; Wightman, R.M. *J. Electroanal. Chem.* **1987**, *220*, 49-63.

8. Amatore, C.; Fosset, B.; Bartelt, J.; Deakin, M.R.; Wightman, R.M. *J. Electroanal. Chem.* **1988**, *256*, 255-268.

9. Oldham, K.B. *J. Electroanal. Chem.* **1988**, *250*, 1-21.

10. Kamau, G.N.; Rusling, J.F. *J. Electroanal. Chem.* **1990**, *292*, 187-198.

11. Pendley, B.D.; Abruña, H.D. *Anal. Chem.* **1990**, *62*, 782-784.

12. Kuwana, T.; Bublitz, D.E.; Hoh, D.E. *J. Am. Chem. Soc.* **1960**, *82*, 5811-5817.

13. Ruff, I.; Friedrich, V.J.; Demeter, K; Csillag, K. *J. Phys. Chem.* **1971**, *75*, 3303-3309.

14. Morris, R.B.; Fischer, K.F.; White, H.S. *J. Phys. Chem.* **1988**, *92*, 5306-5313.

FIGURES.

1. Cyclic votammograms for the oxidation of ferrocene in acetonitrile at a 2.4 μm radius Pt disk electrode. (A) 1.1mM Fc in 0.1M TBAP; (B) 0.97 mM Fc in 10μM TBAP; (C) 1.3 mM Fc in 1 μM TBAP; (D) 1.5 mM Fc in 0.2 μM TBAP; (E) 1.0 mM Fc in 4 nM TBAP. Scan rate = 20 mV/s.

2. Plot of $[E_{1/2}(xs. elec.) - E_{1/2}]$ versus $\ln(C_{redox}/8C_{elec})$ for the oxidation of ferrocene in acetonitrile using 2.4 (□), 12.4 (Δ), 21.3 and 22.1 (O) μm radius Pt disk electrodes, and for the reduction of TCNQ in acetonitrile using a 21.3 (●) μm radius Pt disk electrode. The dashed lines correspond to eqs. (34) and (35) and assume a background ion impurity concentration of 40 nM for the ferrocene and 260 nM for the TCNQ. The solid line assumes an impurity level of 80nM for ferrocene and a diffusivity of ferrocene which is twice that of ferricenium. Representative error bars are shown.
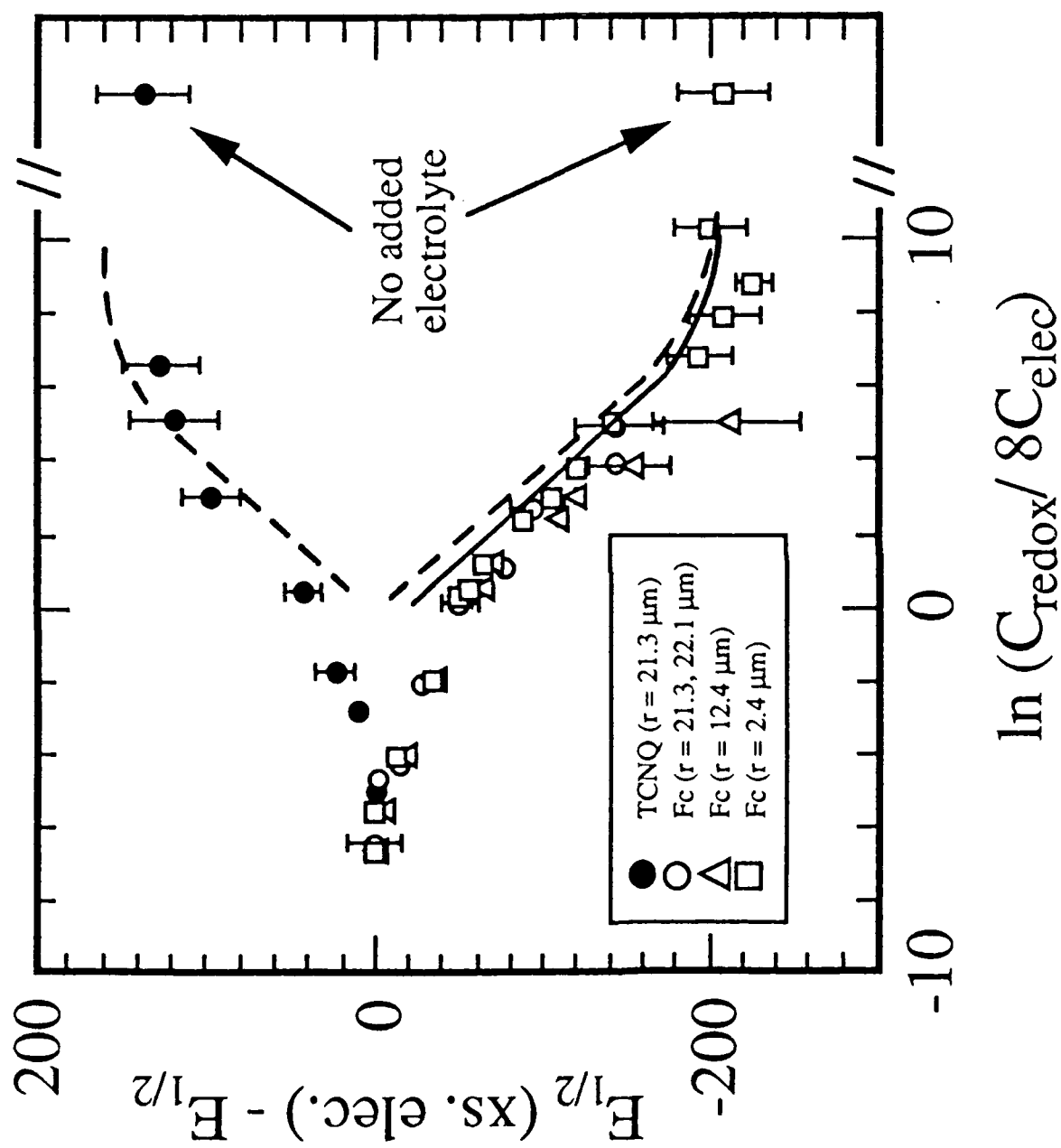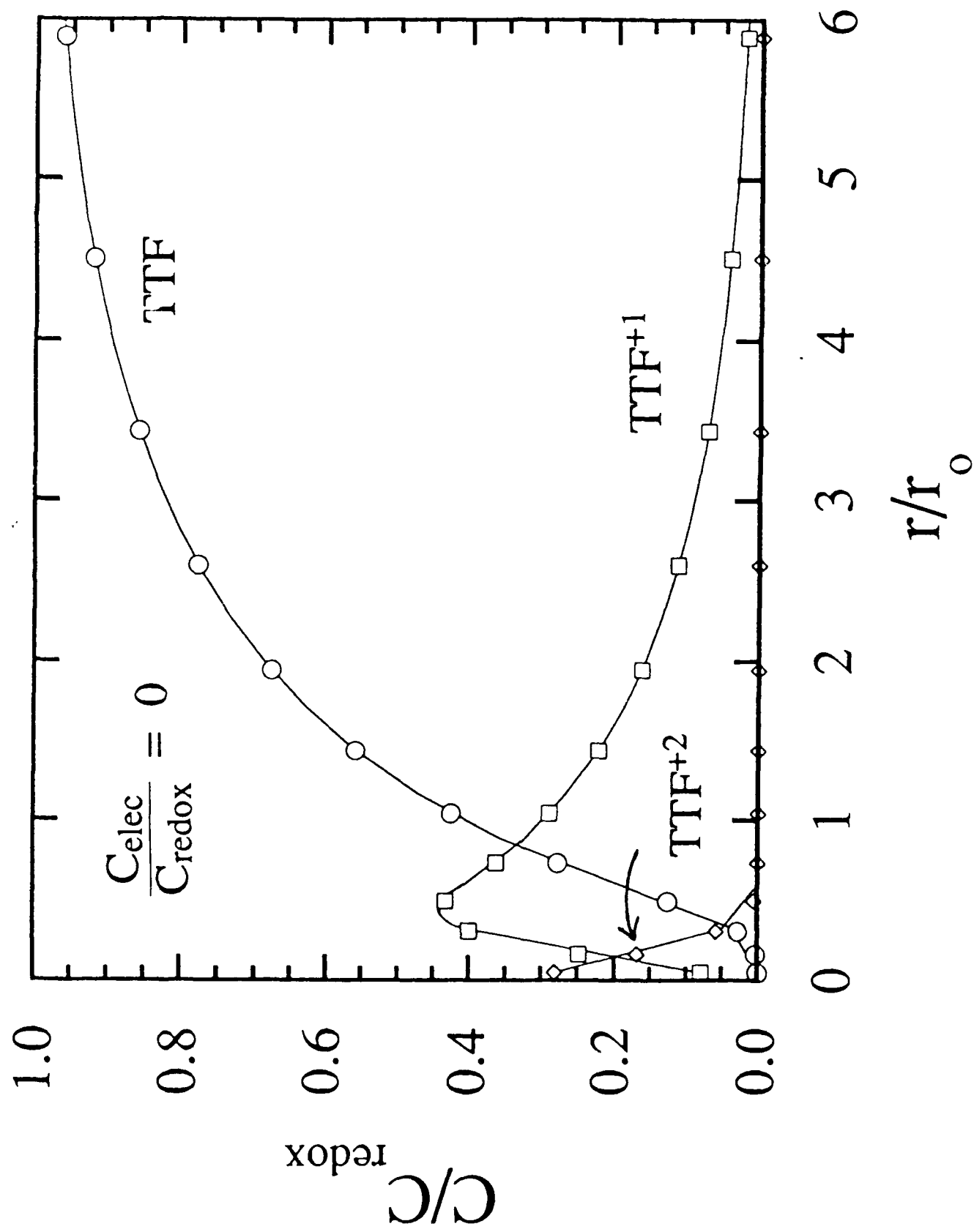
1nA

A

B

C

D

E

+1.00   +0.80   +0.60   +0.40   +0.20   0.0

E vs. SSCE

Fig. 1

Fig. 3

Fig. 4 (Bottom)